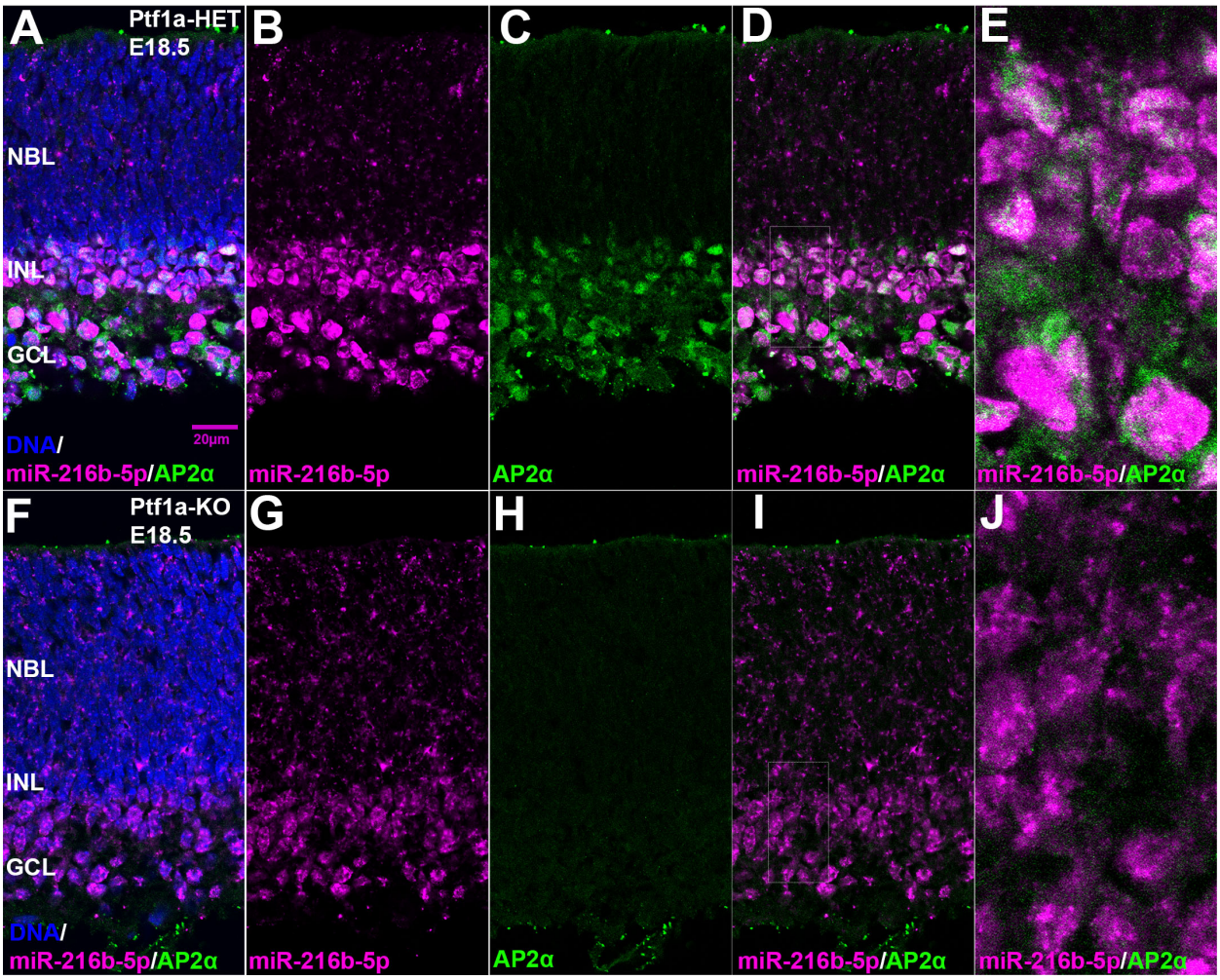

Fig. S1. **miR-216b expression in amacrine cells in E18.5 retinas.** (A-E) Mature miR-216b detected by fluorescent in situ hybridization (magenta) overlaps with AP2α (green) in retinas from mice heterozygous for Ptf1a.(F-J) Expression of mature miR-216b is reduced in the INL/GCL and AP2α is absent in retinas from mice homozygous for disruption of Ptf1a. (E) and (J) show enlargement of regions indicated in (D) or (I). Blue: nuclear DNA.

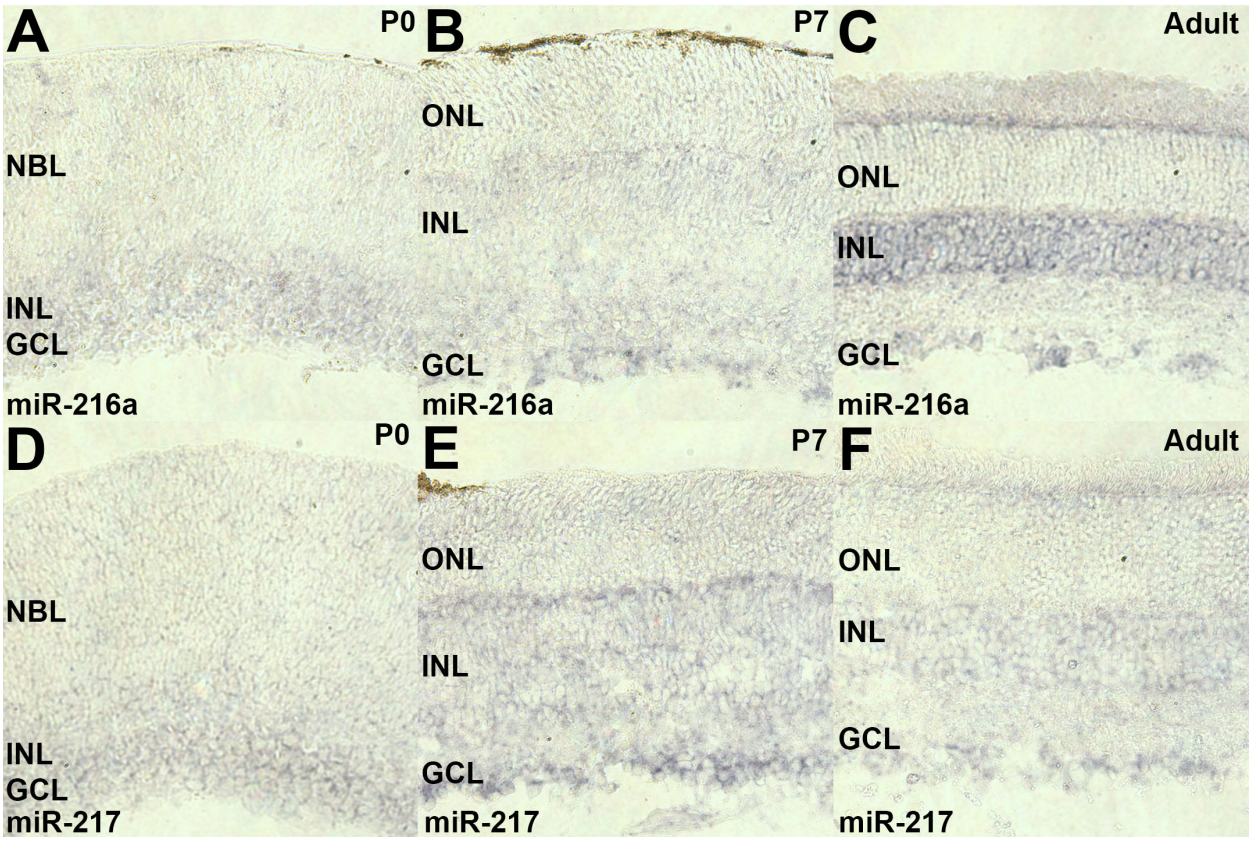

Fig.S2. **miR-216a and miR-217 expression in retina.** (A-C) Mature miR-216a detected by in situ hybridization (purple) is present in INL and GCL of P0, P7, and adult retinas. (D-F) Mature miR-217 is present in INL and GCL of P0, P7, and adult retinas.

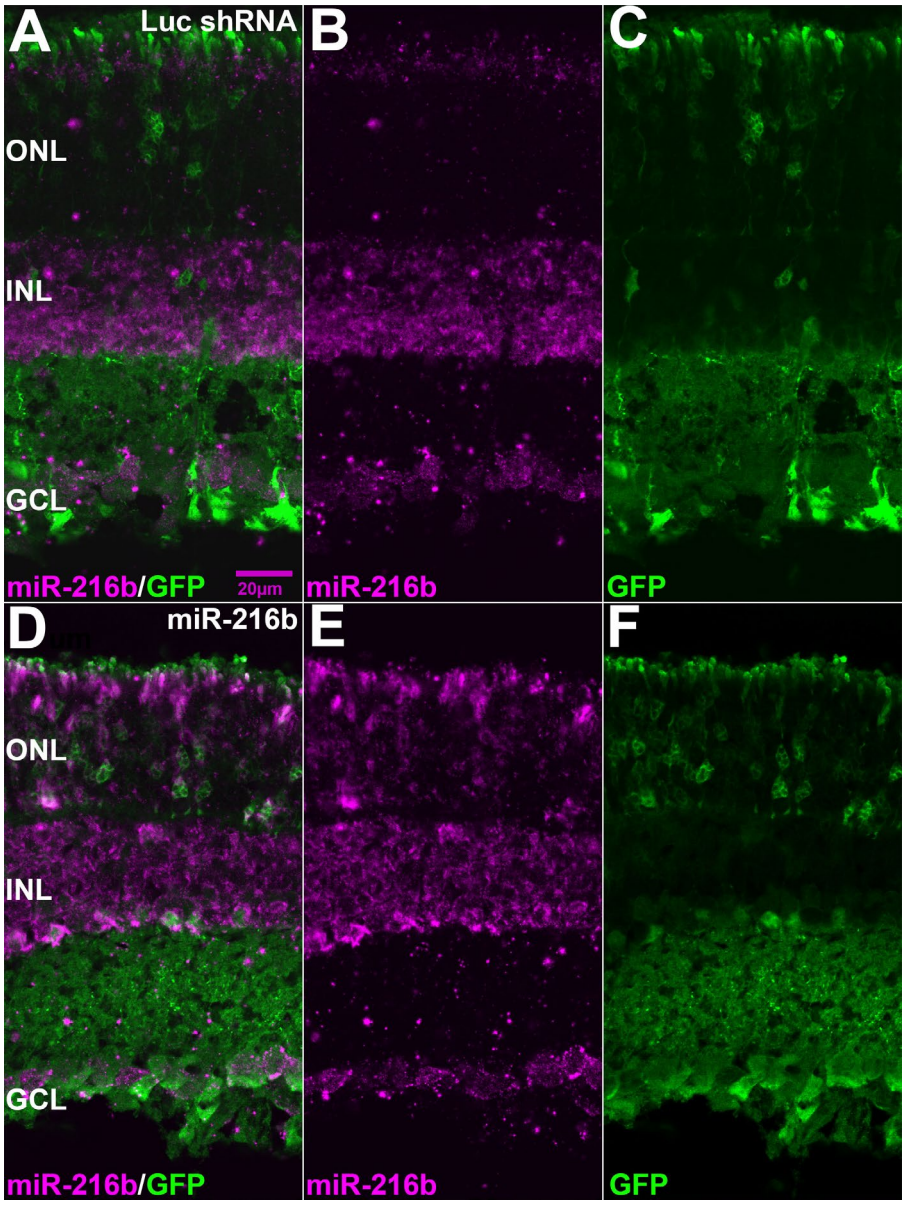

Fig. S3. **Detection of ectopic expression of the miR-216b miRNA in the mouse retina.** Plasmid vectors that co-express GFP with either miR-216b or a control Luc shRNA were introduced into the retina by *in vivo* electroporation at P0; retinas were fixed at P12 and processed in situ hybridization to detect mature miR-216- 5p (magenta) and indirect immunofluorescence to detect GFP (green). (A-C) In control retinas, widespread GFP-labeled cells are present in the ONL and INL, but high-level miR-216b-5p expression is restricted to the INL and GCL (sites of endogenous miR- 216b-5p expression) and low or absent in rods in the ONL. (D-F) In retinas electroporated with the miR-216b expression vector, ectopic miR-216b is detected in the rods of the ONL.

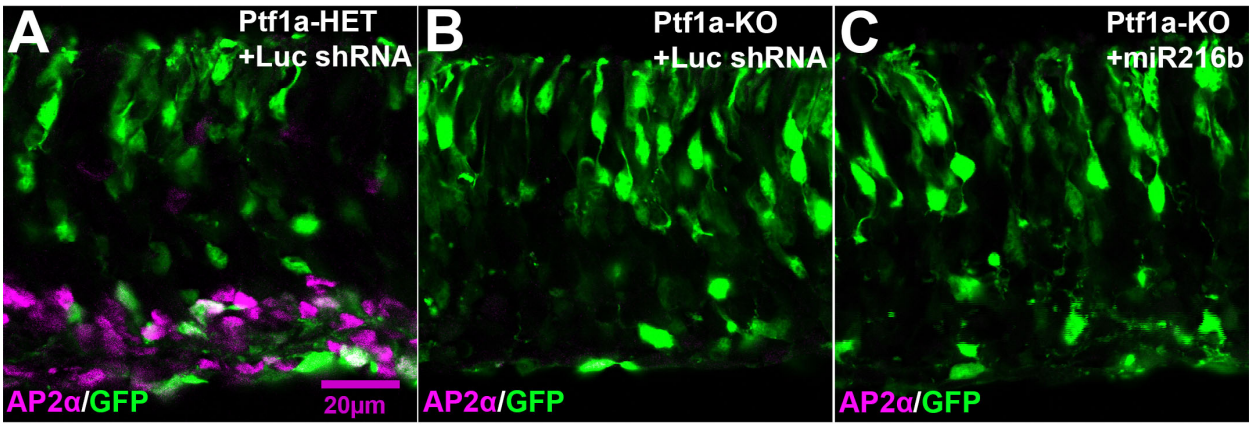

Fig. S4. **Ectopic expression of miR-216b in the developing retina does not generate amacrine cells in retinas from Ptf1a knockout mice.** Plasmid miRNA expression vectors which co-express GFP and either pre-miR-216b or the control Luc shRNA were introduced into retinas at E16.5 by electroporation, then the retinas were maintained in explant culture for 8DIV. (A) Control retina from a Ptf1a heterozygous mouse showing AP2α (magenta) overlaps with a subset of GFP-labeled cells (green). (B, C) In retina explants from mice homozygous for disruption of Ptf1a, AP2α labeled cells were not present among the GFP-labeled cells (representative images, N=3 for each vector in Ptf1a knockout retinas).

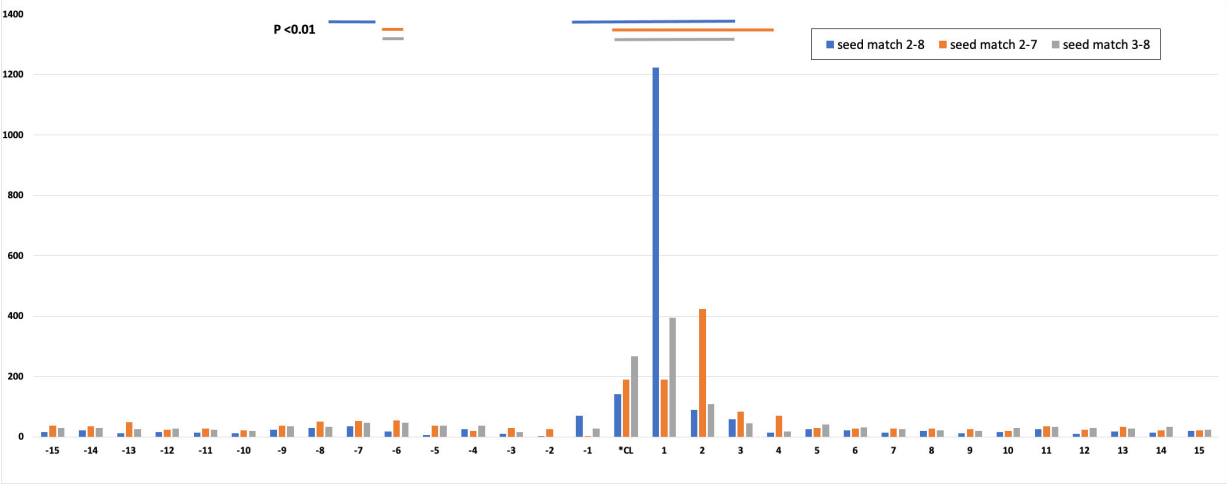

Fig. S5. miRNA seed matches are enriched near the predominant crosslinks in retina Argonaute PAR-CLIP libraries. We mapped common retinal miRNA seed sequences in 31 nt windows around 7237 predominant crosslink sites in 3' UTR exons. Crosslink sites near exon borders were excluded to avoid seed mappings outside of the exons. Seed matches were mapped at the 5' most base of each match, relative to each predominant crosslink site. The graph shows the count of 6 or 7 nt seed matches within +/-15 nt of a predominant crosslink site (*CL), summed across all sites. Only the longest match to a seed was counted (i.e. a 2-7 match or a 3-8 match located within a 2-8 match were not counted). Positions with enrichment ($P < 0.01$; Bonferonni correction used to adjust P values for multiple testing) for each type of seed match are indicated by matching color lines above the graph. Seed matches which overlap the crosslink site must have an A at the appropriate position in the seed to allow basepairing with the crosslinked U in the target, so fewer seeds can map at positions -6 to 0 (=*CL). DNA sequences for the 15 miRNA seeds used: miR-9-5p CTTTGGT, miR- 9-3p AAAGCTA, let-7ifagcdbe-5p/miR-98-5p GAGGTAG, miR-124-3p AAGGCAC, miR- 182-5p TTGGCAA, miR-183-5p ATGGCAC, miR-26ab-5p TCAAGTA, miR-181abdc-5p ACATTCA, miR-30dcaeb-5p GTAAACA, miR-148ab-3p/miR-152-3p CAGTGCA, miR-25-3p/miR-92ab-3p/miR-32-5p ATTGCAC, miR-99ba-5p/miR-100-5p ACCCGTA, miR-93-5p/miR-20a-5p/miR-17-5p/miR-106b-5p AAAGTGC, miR-125ab-5p/miR-351-5p CCCTGAG, miR-7ab-5p GGAAGAC. miRNAs with these seeds are expressed at P0 in the mouse retina (see Supplemental Table S2).

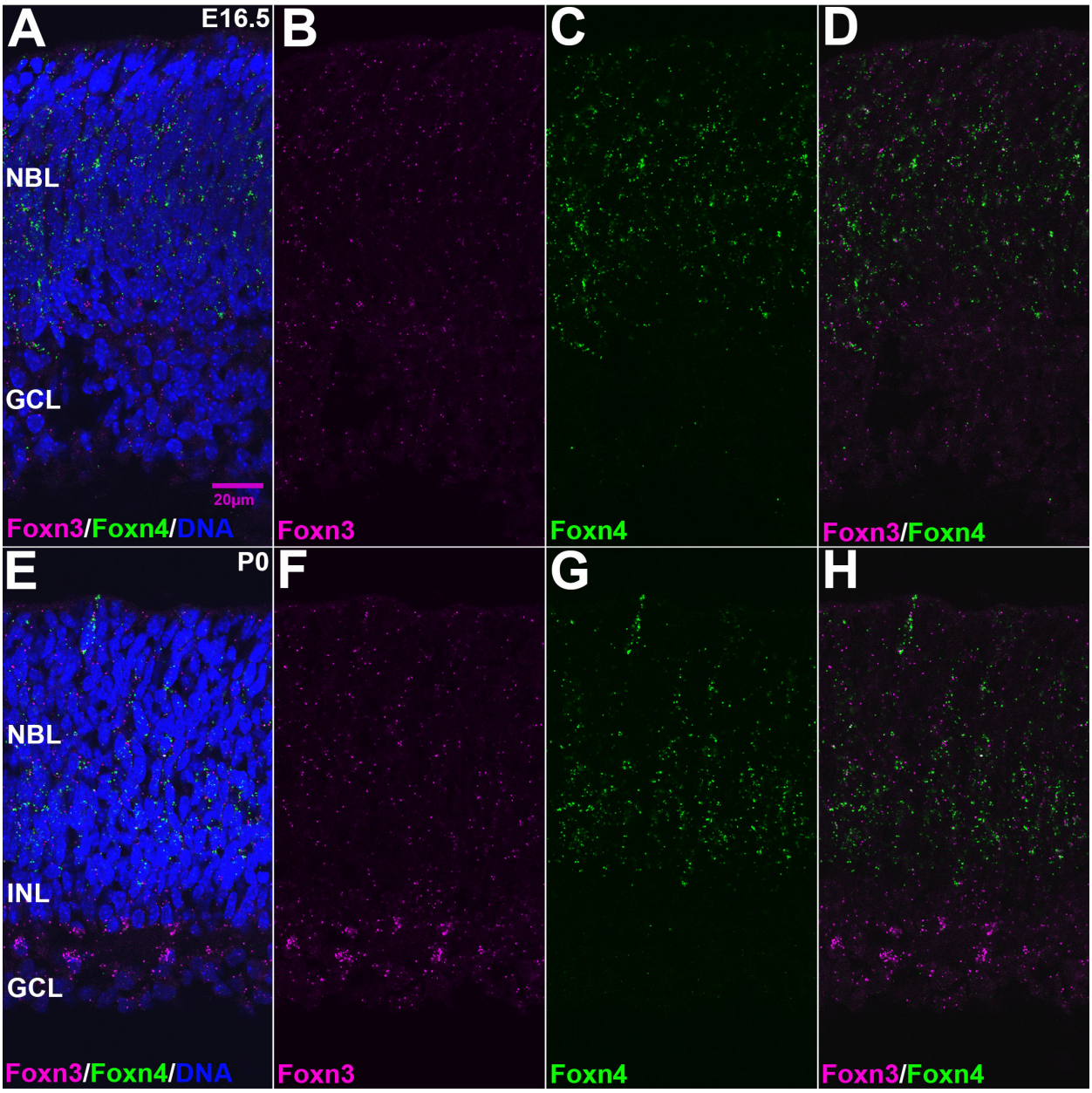

Fig. S6. Overlap between Foxn3 and Foxn4 expression in the developing retina.

(A-D) Foxn3 (magenta) and Foxn4 (green) expression in cells of the E16.5 retina, detected by in situ HCR. (E-H) Complete panels for Foxn3 and Foxn4 expression detected by in situ HCR in the P0 retina; Panel H is the same as Fig. 4G. Blue in A and E: nuclear DNA.

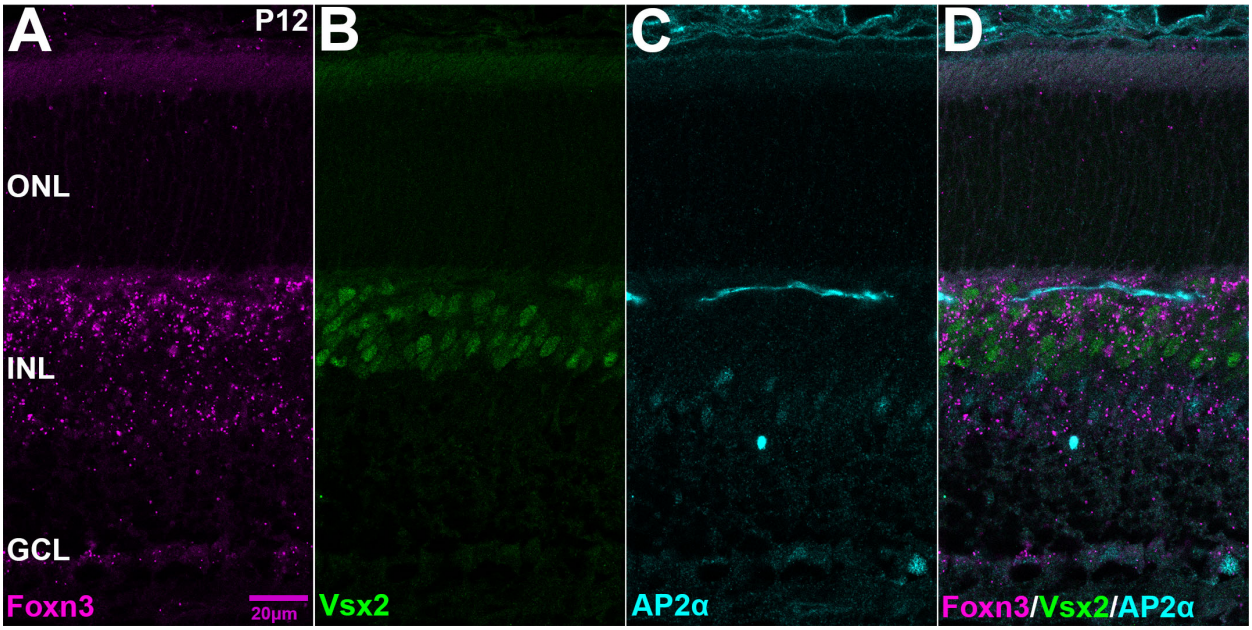

Fig. S7. Complete panels for Foxn3 and marker expression in the P12 retina. (A-D) Foxn3 mRNA in the INL at P12 (magenta), detected by in situ HCR, overlaps with Vsx2 (green) and AP2α (cyan) detected by immunofluorescence. Panel D is the same as Fig. 4L.

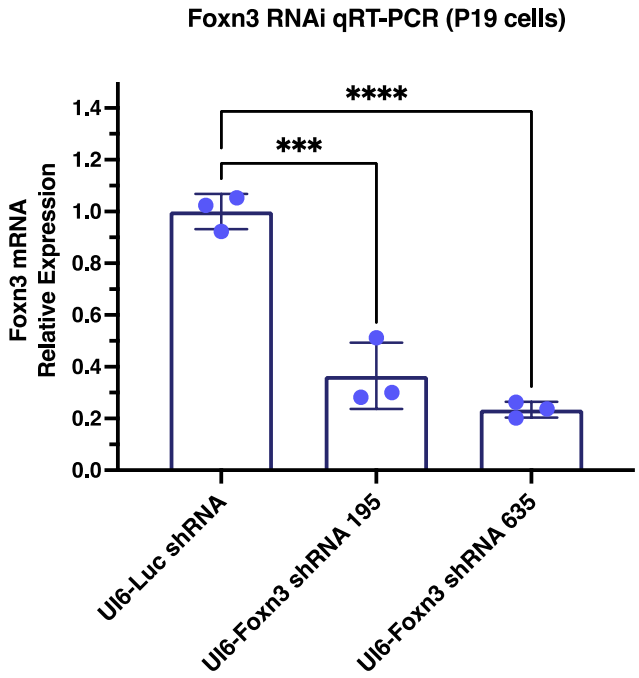

Fig. S8. Foxn3 RNAi reduces Foxn3 mRNA in a cell line. Mouse P19 cells were transfected with the control Luc-shRNA vector or one of two Foxn3 shRNA vectors. Foxn3 mRNA was measured by qRT-PCR. Both Foxn3 shRNAs reduced endogenous Foxn3 mRNA relative to the control (N=3). Significance based on one-way ANOVA with Dunnett's multiple comparisons test: *** $P < 0.001$, **** $P < 0.0001$. Graphs show mean ± s.d.

A

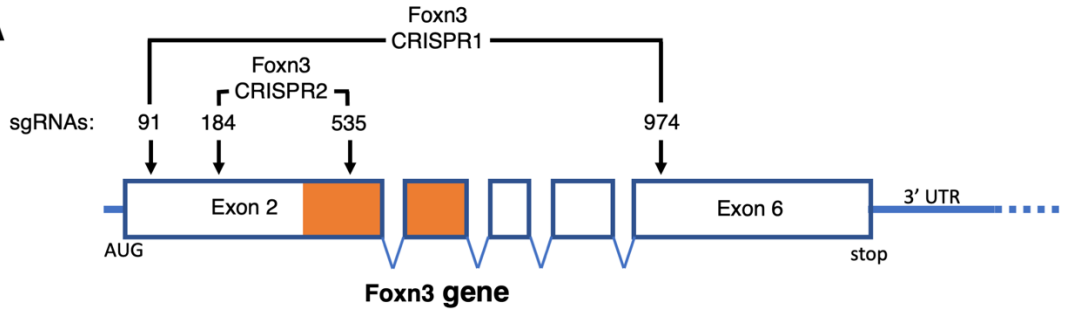

B

Foxn3 CRISPR1	Indel	Aligned Reads
sgRNA 91	0.69%	112,556
sgRNA 974	5.91%	47,513
control (91 target)	0.01%	48,440
control (974 target)	0.02%	44,292
Foxn3 CRISPR2		
sgRNA 184	0.01%	64,309
sgRNA 535	5.84%	57,015
control (184 target)	0.01%	69,888
control (535 target)	0.01%	58,123

Fig. S9. **CRISPR in retinal explants disrupts the Foxn3 gene.** (A) Schematic showing the location of sgRNA target sites within the coding exons of the Foxn3 gene on mouse Chr12. Orange indicates the Forkhead domain; introns are not to scale. Each CRISPR plasmid expresses two different sgRNAs as indicated. The 91 and 535 sgRNAs also match a Foxn3 pseudogene on mouse ChrX. The pseudogene does not appear to be expressed (no mRNA/EST sequences) and the coding potential of the pseudogene is disrupted by multiple frameshifts and mutations. (B) E16 retina explants were electroporated with a Foxn3 CRISPR vector or the parental CRISPR vector control. Genomic DNA was isolated two days later. Each of the four sgRNA target regions were PCR amplified and analyzed by Illumina sequencing. The number of reads and percentage of insertions/deletions (Indel) is listed for each sgRNA target site. For each of the two Foxn3 CRISPR vectors, one of the two sgRNAs was effective at generating indels. See Supplemental Table S6 for sequence alignments at each site.

Table S1. miRNA counts for small RNA seq of E16.5 retinas from mice heterozygous or homozygous for disruption of Ptf1a.

Click here to download Table S1

Table S2. miRNA counts for small RNA seq of P0 retinas from wild-type CD-1 mice.

Click here to download Table S2

Table S3. PAR-CLIP crosslink sites with a nearby sequence matching the seed sequences of both miR-216b and miR-216a.

Click here to download Table S3

Table S4. PAR-CLIP crosslink sites with a nearby sequence matching a seed sequence of either miR-216b or miR-216a but not both.

Click here to download Table S4

Table S5. Foxn3 mRNA expression in amacrine single cell RNA-seq data.

Click here to download Table S5

Table S6. Sequence analysis of Foxn3 CRISPR retina target sites.

Click here to download Table S6

Table S7. Sequences of oligonucleotide probes and primers.

Click here to download Table S7